Journal of Thermal Analysis, Vol. 34 (1988) 551–557

HIGH TEMPERATURE STUDY OF THE ZIRCONIUM-RHODIUM SYSTEM

J. L. Jorda, J. C. Gachon, J. Charles* and *J. Hertz*

LABORATOIRE DE THERMODYNAMIQUE MÉTALLURGIQUE,
UA CNRS 1108-UNIVERSITÉ DE NANCY I,
BP 239, 54506 VANDOEUVRE-LES-NANCY, FRANCE
* DPMC — UNIVERSITÉ DE GENÈVE,
24, QUAI E.—ANSERMET, CH 1211 GENÈVE 4, SCHWITZERLAND

High temperature ($T > 1600$ K) part of the phase diagram and calorimetric studies in the binary Zr–Rh system are presented. Five intermetallic compounds: Zr_2Rh, ZrRh, Zr_3Rh_4, Zr_3Rh_5 and $ZrRh_3$ are present in the compositional phase diagram. The enthalpy of formation of Zr_2Rh, ZrRh and $ZrRh_3$ have been measured and refined from an optimization of the phase diagram. A thermodynamic description of the system is proposed.

The discovery by Matthias [1] of superconductivity in the Zr–Rh system constitutes the first cast of numerous investigations. Zegler [2] produced a tentative phase diagram of the Zr-rich field and discovered the metastable Omega phase. Eremenko et al. [3] in a brief study of transition metals systems involving Zr suggested the Rh-rich field of Zr–Rh. Togano and Tachikawa [4] succeeded the amorphization of alloys containing approximately 25 at.% Rh. Despite those efforts, it appears as pointed out by Kuentzler and Waterstrat [5] that the phase relations in the system remain doubtfull.

In addition, except the calculations by Kaufman and Bernstein [6] based on erroneous phase diagram, the thermodynamic functions associated with Zr–Rh phases were unknown.

The aim of this paper is to precise the high temperature relations of the Zr–Rh system and to give the Gibbs energies of formation of the different phases. For this we have used the high temperature efficient techniques in our respective laboratories: differential thermal analysis (DTA) up to 2600 K, thermal analysis on levitation samples [7–9], and direct quantitative calorimetry up to 1800 K [10, 11]. Solidus lines in the total concentration range and enthalpies of formation of Zr_2Rh, ZrRh and $ZrRh_3$ allowed us to refine the thermodynamic functions of these compounds and to estimate those of Zr_3Rh_5 and of the liquid phase.

John Wiley & Sons, Limited, Chichester
Akadémiai Kiadó, Budapest

I. Experimental

I. 1. Sample preparations

Mixtures of Zr ingots (3N, UMC) and Rh (3N, Johnson–Matthey) were arc-melted in an argon atmosphere. The starting Rh powder was premelted in order to avoid further sputtering during mixing. The macroscopic homogeneity of the samples was improved by 3 consecutive melts. The total weight losses were less than 0.5% thus indicating the concentration uncertainty. The alloys were submitted to high temperature anneal: 60 hours at 1273 K for Rh-poor concentrations and 50 hours at 1775 K for Rh content more than 50 at%.

Samples appointed to calorimetric investigations were compacted in a glove-box under purified argon atmosphere from Zr(3N, Ventron) and Rh(4N, Aldrich) 180 and 150 micrometers size powders, respectively. The Rh content of the mixtures were 36, 53 and 77.2 weight percent which corresponded to the compounds Zr_2Rh, ZrRh and $ZrRh_3$, respectively. The compacted pellets were stored under Ar and reaction in the calorimeter was performed a few hours after compaction in order to avoid further oxygen absorption.

I. 2. Thermal analysis

Melting temperature of 30 alloys covering all the concentration scale were measured using two independent methods: DTA and thermal analysis on samples heated in a levitation coil. The details and procedures are reported in previous publications [7–9]. We recall here that our DTA cell is BeO based material. The temperature of the cell and the differential temperature are measured by W–3%Re vs. W–25% Re thermocouples. Systematic calibrations ascertain an accuracy of 20 K at 2000 K. The system is able to operate up to 2600 K.

Thermal analysis on levitating samples are based on the modification of the radius of the samples when a solidus line is crossed. This involves a change in the position of the sample in the levitation coil. As a consequence, the temperature of the alloy, measured with a two-color pyrometer suddenly increase. The accuracy is about 10 K at 2000 K.

I. 3. Calorimetry

The calorimetric system was extensively described by Gachon et al. [10, 11]. Compressed disks of a few milligrams are dropped in the calorimetric cell heated at a constant temperature which depends on the alloy under investigation. For Zr_2Rh

and $ZrRh_3$ this temperature was 1423 K but it had to be increased up to 1700 K to improve complete reaction for ZrRh. For each alloy, 10 independent measurements were performed after calibration with pure alumina. The standard deviation was approximately 4%.

I. 4. X-Ray

Among the systematic methods used to control the samples quality, the X-Ray powder diffraction of each alloy was analysed. We used the Guinier method with the Cu K-alpha radiation. Si, as internal standard, was added to the powders.

II. Results

II. 1. Phase diagram

Figure 1 represents the high temperature part of the phase diagram of Zr–Rh as deduced from the analysis described in the preceding section. The study is voluntary

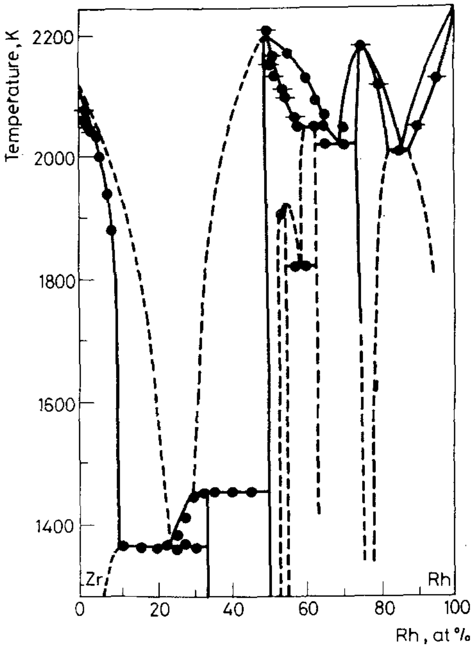

Fig. 1 Schematic experimental phase diagram of the Zr–Rh system.
● Differential thermal analysis;
–●– Thermal analysis on levitating samples

restricted to solid-liquid equilibrium which allows liquidus computation according to Charles' method [12]. A complete version of the phase equilibria, combined with occurence of superconductivity will be published elsewere [13]. Nevertheless it is interesting to note some peculiarities which are discussed in the following.

— The β–Zr solid solution extends up to 9 ± 1 at.% Rh. at the eutectic temperature (1353 ± 5 K). The concentration of the liquid at the eutectic point is 23 at.% Rh. The lattice parameter of the cubic cell of β–Zr decreases from 3.610(3) Å for pure Zr to 3.510 Å for 8 at.% Rh.

— Zr_2Rh is a peritectically reacted compound formed at 1440 ± 5 K, at the stoichiometric ratio 2 : 1. This, unambiguously confirms the assumption of Zegler [2]. The homogeneity range is restricted to less than 1 at%. No change in the cell volume and the unmodified superconducting transition temperature (11.2 K) when the concentration changes support this affirmation. The cell is of tetragonal symmetry, $CuAl_2$-type structure with $a = 6.488(3)$ Å, $c = 5.608(3)$ Å in agreement with Zegler's results [2].

— For Rh concentrations ranging from 50 to 65 at.% some discrepancies appear in the literature, which concern the number and the structure of the possible phases. We have found that stoichiometric ZrRh congruently melts at 2210 ± 10 K. The solidus extends up to more than 60 at.% Rh, thus suggesting a large high temperature homogeneity range.

A compound corresponding to the Zr_3Rh_4 stoichiometry is formed from solid state decomposition of the ZrRh phase at 1930 K. A temperature invariant at 2060 ± 20 K was revealed, presumably due to the peritectic formation of Zr_3Rh_5, a compound first mentioned by Raman and Schubert [14] but assumed by Kuentzler and Waterstrat [4] to result from a martensitic transformation of ZrRh. Our observations on crystallographic structure disagree with the NbRu-type structure assumed by Raman and Schubert [15]. Efforts on structure determination are under work.

The high temperature structure of ZrRh is of the CsCl type accordingly with Raman and Schubert [14] and Eremenko et al. [15] results. The lattice parameter of $Zr_{46}Rh_{54}$ was $a = 3.255$ Å a value lower than this reported by Eremenko et al. [16]. At 923 K the equiatomic ZrRh undergoes a martensitic transformation. The low temperature modification of ZrRh has presumably an orthorhombic symmetry, FeB-type structure.

— $ZrRh_3$ congruently melts at 2180 ± 10 K. At the eutectic temperature (2013 ± 20 K) the phase extends up to 80 at.% Rh. The well known Cu_3Au type structure [15] is confirmed. For quenched samples from 1273 K, the lattice parameter changes from 3.928(3) Å to 3.887(1) Å (70 to 78 at.% Rh).

— The maximum solubility of Zr in Rh is 12 at.% at 2013 K.

The limit of solubility rapidly decreases with the temperature down to 1 at.% at 1273 K.

— In addition to these phases which enter into equilibrium with the liquid phase, a special mention concerns Zr_3Rh_4. The compound is formed from solid state reaction at about 1973 K and undergoes a martensitic transformation.

Table 1 Thermodynamic functions of formation and melting of phases in the Zr–Rh system. Reference states: β-Zr*, (bcc) and Rh*(fcc)

Stoichiometry	Enthalpies of formation, J/mol				
			Phase diagram optimization		
	Direct calorimetry	Estimation Kaufman Bernstein	$\Delta_f H$, J/mol	$\Delta_f S$ J/mol K	$\Delta_m S$
$Rh_{.33}$ $Zr_{.67}$	−55400 (σ=2000) at 1423 K		−54029	−15.1	12.8
$Rh_{.50}$ $Zr_{.50}$	−75800 (σ=5000) at 1700 K		−78807	−23.1	8.3
$Rh_{.625}$ $Zr_{.375}$	not measured	−88000 $ZrRh_2$ at 300 K	−86277	−29.8	9.0
$Rh_{.75}$ $Zr_{.25}$	−77700 (σ=4000) at 1423 K −71800 (σ=3000) at 1700 K	−74000 at 300 K	−68644	−24.5	4.0

Liquid: reference states = liquid Zr* and Rh*.
$g^E = x(1-x)[-326\,109 + 121.15T + (-214\,696 + 128.58T)(2x-1)]$.

II. 2. Thermochemistry

We have reported in table 1 the enthalpies of formation of Zr_2Rh, ZrRh and $ZrRh_3$ as measured at high temperature. The experimental values are compared with the calculations of Kaufman and Bernstein [6]. Remembering that the later were obtained from erroneous phase diagram, and that we have no experimental data on Zr_3Rh_5, comparison is restricted to $ZrRh_3$. The results are rather in good agreement.

Optimized values of the thermodynamic functions were computed using a program described by Charles [12]. The excess Gibbs-energy of the liquid phase is modelised by a polynomial development of the third degree in x and first degree in T, on the basis of Legendre's orthogonal functions. Each compound is introduced

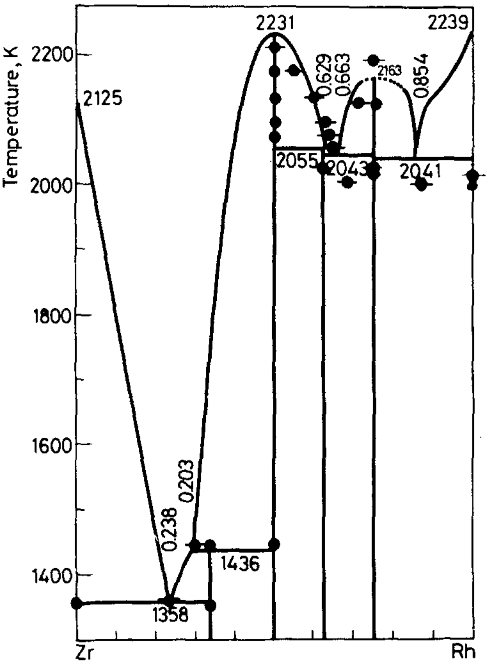

Fig. 2 Zr–Rh phase diagram as computed using Charles' method

in the program as a stoichiometric compound with constant enthalpy and entropy of formation according to the Kopp–Neumann's approximation. The adjustable parameters of the optimization process are the four coefficients of the polynomial development and the eight enthalpies and entropies of formation of the compounds (see table 1). Optimization is based on the solution of an overdeterminated set of linear equations taking into account:

i. the three experimental calorimetric values of $\Delta_f H$ for the three compounds studied (only as proposal values in the overdeterminated system),

ii. seventeen conditions of equilibrium between liquid and solid phases, as located by circles on Fig. 2.

iii. enthalpies and entropies of melting of the pure components as fixed values.

The actual version of the program does not take into account the extended solid solutions. For this reason, we encountered here some difficulties to reproduce the experimental liquidus as can be see in Fig. 2. Optimized values are reported in Table 1. Complete coherence was not yet obtained, specially in the Rh-rich field of the diagram.

Conclusion

The phase diagram of the zirconium–rhodium system was investigated at high temperature, showing some significant modifications to previous versions. The direct measurement of the enthalpies of formation of Zr_2Rh, ZrRh and $ZrRh_3$ allows us to propose a tentative of coherent thermodynamic description of this binary system.

References

1 B. T. Matthias, Physical Review Letters, 97 (1955) 74.
2 S. T. Zegler, Phys. Chem. Solids, 26 (1964) 1347.
3 V. M. Eremenko, E. L. Semenova and T. D. Shmena, Metallofizika, 52 (1974) 112.
4 K. Togano and K. Tachikawa, J. of the Less Common Metals, 33 (1973) 275.
5 R. Kuentzler and R. M. Waterstrat, Solid State Communication, 54 (1985) 517.
6 L. Kaufman and H. Bernstein, Comp. Calc. Phase Diagrams with special reference to Refractory Metals, Acad. Press, NY 1970 p. 148.
7 J. L. Jorda, R. Fluckiger and J. Muller, JCAT X – Marseille 1979, HT5.
8 R. Fluckiger and J. L. Jorda, Application of phase diagrams in metallurgy and ceramics, Vol. I NBS Special publication 496 (1978) 375.
9 J. L. Jorda, R. Fluckiger and J. Muller, J. Material Sci., 13 (1978) 2471.
10 J. C. Gachon, M. Notin and J. Hertz, JCAT X – Marseille 1979 HT2.
11 J. C. Gachon and J. Hertz, Calphad, 7 (1983) 1.
12 J. Charles, J. C. Gachon and J. Hertz, Calphad, 9 (1985) 35.
13 J. L. Jorda, T. Graf, L. Schellenberg, J. Muller, K. Cenzual, J. C. Gachon and J. Hertz, J. Less Common Metals, 136 (1988) 313.
14 A. Raman and K. Schubert, Z. Metallkunde, 55 (1964) 704.
15 V. N. Eremenko, E L. Semenova, T. D. Shmena and V. Kudrjavtsev, Dopovidi Akad. Nauk, 10A (1978) 943.

Zusammenfassung — Der Hochtemperaturteil ($T > 1600$ K) des Phasendiagramms des binären Systems Zr—Rh und die Ergebnisse diesbezüglicher kalorimetrischer Messungen werden mitgeteilt. Fünf intermetallische Verbindungen (Zr_2Rh, ZrRh, Zr_3Rh_4, Zr_3Rh_5 und $ZrRh_3$) treten im Phasendiagramm auf. Die Bildungsenthalpie von Zr_2Rh, ZrRh und $ZrRh_3$ wurde bestimmt und durch Optimierung des Phasendiagramms verfeinert. Eine thermodynamische Beschreibung des Systems wird gegeben.

Резюме — Представлены высокотемпературная ($T > 1600$ K) часть фазовой диаграммы и калориметрические исследования двойной системы Zr—Rh. На сложной фазовой диаграмме идентифицированы пять интерметаллических соединений Zr_2Rh, ZrRh, Zr_3Rh_4, Zr_3Rh_5 и $ZrRh_3$. Измеренные энтальпии образования фаз Zr_2Rh, ZrRh и $ZrRh_3$ были уточнены на основе оптимизации фазовой диаграммы. Предложено термодинамическое описание данной системы.